

# Bending of a Cross-Ply Laminated Composite Beam Under a Sinusoidal Transverse Loading

Fatih Karaçam 

Trakya University, Department of Mechanical Engineering, Edirne, Türkiye

## ABSTRACT

Bending of a laminated composite beam under to a sinusoidal loading is carried out for simply support boundary condition for a specific cross-ply stacking sequence. To demonstrate the accuracy of the analytical results, a computer-aided engineering (CAE) approach is used. In the analytical solution, a unified shear deformation theory with a parabolic shape function is used. The longitudinal and vertical displacements, normal and shear stresses, namely, the bending stresses of analytical and CAE solutions are obtained and compared with the literature. Although two different methods are used in the study, the analysis results converge to the reference values. The variation of the displacements, normal and shear stresses are illustrated in the graphics with respect to the beam length and thickness respectively.

### Keywords:

Bending; Static analysis; Laminated composite beam; Shear deformation beam theory; Computer-aided engineering

### Article History:

Received: 2023/04/10

Accepted: 2023/10/27

Online: 2023/12/31

Correspondence to: Fatih Karaçam,

E-Mail: fatihkar@trakya.edu.tr

Phone: +90 284 226 1226 (1217)

Fax: +90 284 226 1218

This article has been checked for similarity.



This is an open access article under the CC-BY-NC licence

<http://creativecommons.org/licenses/by-nc/4.0/>

## INTRODUCTION

Since the composite materials can be designed in different ways with the desired mechanical properties for various stacking sequences, matrix and fiber materials, they have been widely used in many structural elements. These elements are generally constructed of laminated composite materials, and too many design parameters are taken into consideration in the design and analysis process. Sankar (2001) obtained an elasticity solution for laminated beams under sinusoidal loading. The stresses and displacements were obtained by use of a non-dimensionalized design parameter that varies exponentially for constant mechanical properties [1]. Sayyad et al (2014) performed a static flexural analysis of a simply supported single-layer composite beam under various loadings and obtained the results by a precise elasticity solution [2]. Sayyad et al (2015) investigated the bending of composite beams by use of a trigonometric beam theory due to transverse shear deformation, and compared the results with those of the other trigonometric theories [3]. Pimenta et al (2015) investigated the sinusoidal-web beams under the effects of lateral and torsional buckling. In this manner, firstly, an experimental investigation was performed, and then a finite-element model was created and tested using the data from the experiments. In the prediction of the beam resistance, a theoretical model was proposed, and a computational program was established. Finally, using the first order reliability

approach, reliability analyses were performed, and the results were compared with the literature [4]. Pagani et al (2017) developed the static analyses of sandwich, and laminated beams under a transverse sinusoidal loading by applying the Lagrange expansion-based refined beam model for a simple supported boundary condition. The 3-D FEM (Finite Element Method) results were computed and compared with the previous studies [5]. Jiao et al (2017) investigated the effect of geometry of composite I-beams for the buckling capacity theoretically, and in order to validate the theoretical approach, number of experiments and simulations were carried out [6]. Liu et al (2018) searched the non-linear bending behavior of anisotropic composite beams for different distributed loadings and compared the results with FEM solution [7]. Dorduncu (2019) investigated the bending stresses of composite beams by use of a refined zigzag theory. The method's capabilities and robustness were presented for various sets of aspect ratios and boundary conditions [8]. Karakoti and Kar (2019) examined the sinusoidally-corrugated laminated composite panels by use of a customized computational code to obtain the bending responses of panels for various boundary conditions. The model's accuracy was confirmed with the comparison and validation of the analytical results [9]. Pandey and Gadade (2019) used FEM in the static analysis of a composite beam. As a present model, the nine-noded, 12-degree-of-

### Cite as:

Karacam F, "Bending of a Cross-Ply Laminated Composite Beam Under a Sinusoidal Transverse Loading". Hittite J Sci Eng. 2023;10 (4): 301-307. doi:10.17350/hjse19030000319

freedom isoparametric Lagrange interpolation function was developed. To compare the FEM results with the literature, the maximum non-dimensional deflection values for symmetric and unsymmetric laminates under concentrated loads were calculated for various boundary conditions [10]. By taking into account four different carbon nanotube distributions, Sobhy (2019) introduced a novel analytical method for the bending of functionally graded plates reinforced with single-walled carbon nanotube in different temperature conditions. For simply supported boundary condition, the present plate was subjected to various distributed loadings, and non-dimensionalized stress and displacement values were obtained [11]. In the bending and vibrational analysis of reinforced beams, Wang et al. (2019) suggested a 2-D (Two-Dimensional) elasticity model for a sinusoidal distributed load and various boundary conditions, non-dimensionalized displacement, stress, and natural frequency parameters were derived [12]. Pathirana and Qiao (2019) investigated the critical buckling load of sinusoidal panels under simply support boundary condition by use of Rayleigh-Ritz method. To predict the critical load, a semi-analytical solution was used, and due to the finite element analysis, the results were obtained with better correlation. Considering the twisting capacities and different material properties, the study was conducted to assess the effects of the buckling amplitude, thickness, and aspect ratio [13]. Pathirana and Qiao (2020) studied the buckling behaviour sinusoidal panels under in-plane loading by Rayleigh-Ritz approach. The local buckling load is predicted accurately by a precise solution method. The local buckling behavior were captured at any aspect ratios, thickness, and amplitudes [14]. Zaboony and Jassim (2022) used the classical lamination theory to obtain the analytical solutions for laminated composite beams. In the analytical bending solution, several boundary conditions and loadings were taken into consideration. The boundary conditions were chosen as simple-simple, clamped-free and clamped-clamped, and the loading types were chosen at the center point with uniform distributed load [15]. Zhu et al (2022) investigated the properties of engineered cementitious composites due to the ductility, strength, fatigue and cracking behavior. To examine the impacts of various fiber contents, three different types of hybrid designed cementitious composites with various volume fractions of steel and polyethylene fiber were evaluated [16].

In the present work, the bending analysis of a cross-ply laminated composite beam under a uniform sinusoidal transverse loading for simple support boundary condition is performed both analytically and by use of a CAE software. For the comparison purposes, initially, the longitudinal and vertical displacements, normal and shear stresses are

obtained analytically for a specific material, at different points where the maximum displacements and stresses may occur. The computer aided engineering approach is developed for given parameters, and the results are compared with the ones obtained by use of finite element method and analytically by use of a shear deformation beam theory in the literature [20-21].

### ANALYTICAL MODEL

The beam is assumed to have a rectangular cross-section and constructed of linear elastic layers. It has a length of "L", total thickness of "h", unit width, and the coordinate axes are located at the mid-plane where  $0 \leq x \leq L$  and  $-h/2 \leq z \leq h/2$ , respectively. A laminated composite beam under a uniform sinusoidal transverse loading is presented in Fig.1.

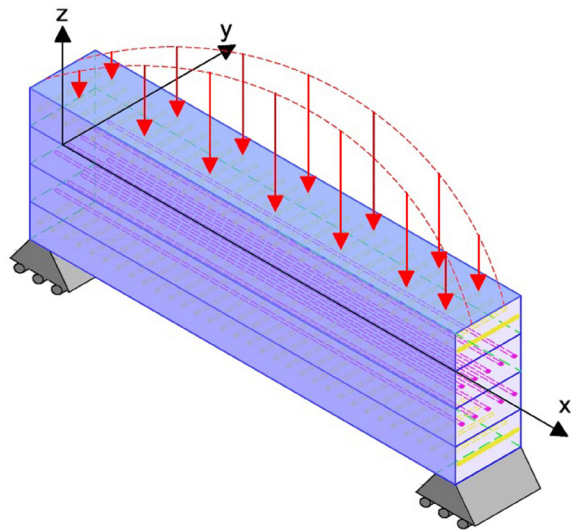


Figure 1. A laminated composite beam under a uniform sinusoidal transverse loading

In the analytical solution, a unified shear deformation beam theory is used which is firstly applied to the composite shells developed by Soldatos and Timarcı (1993). The shear deformation effects are taken into consideration by use of a general shape function " $\phi(z)$ " depending on the beam thickness. In addition, with the appropriate selection of the shape functions, the previous beam theories can also be obtained. The displacement fields for the unified shear deformation beam theory are given as follows:

$$\begin{aligned}
 U(x, y, z; t) &= u(x, y; t) - z w(x; t)_{,x} + \phi(z) u_1(x; t) \\
 V(x, y, z; t) &= v(x, y; t) - z w(x; t)_{,y} + \phi(z) v_1(x; t) \\
 W(x, y, z; t) &= w(x, y; t)
 \end{aligned}
 \tag{1}$$

Since the displacement component along y-axis is zero for the beam, the following displacement fields "U" and "W" are obtained as follows, where "u", "w" and "u<sub>1</sub>" are the displacement functions of the mid-plane.

$$U(x, z; t) = u(x; t) - z w(x; t)_{,x} + \mathcal{O}(z) u_{1,x}(x; t) \quad (2)$$

$$W(x, y, z; t) = w(x, y; t)$$

In order to satisfy the stress-free conditions at the top and bottom surfaces and continuity of interlaminar stresses through the thickness of the beam, a parabolic shape function is chosen in the study as follows [17]:

$$\mathcal{O}(z) = z \left( 1 - \frac{4z^2}{3h^2} \right) \quad (3)$$

The displacement fields given in Eq. 2 yield to the kinematic relations where the subscript “,” corresponds to the differentiation with the relevant axis.

$$\varepsilon_x = u_{,x} - z w_{,xx} + \mathcal{O}(z) u_{1,x} \quad (4)$$

$$\gamma_{xz} = \mathcal{O}'(z) u_1$$

Using the generalized Hooke's law, the stress-strain relations in each layer of the beam can be expressed as follows:

$$\begin{bmatrix} \sigma_x \\ \tau_{xz} \end{bmatrix} = \begin{bmatrix} \bar{Q}_{11} & 0 \\ 0 & \bar{Q}_{55} \end{bmatrix} \begin{bmatrix} \varepsilon_x \\ \gamma_{xz} \end{bmatrix} \quad (5)$$

The transformed reduced stiffness “ $\bar{Q}_{ij}$ ” depend on the reduced stiffness “ $Q_{ij}$ ” and fiber orientation angles “ $\theta$ ” of the relevant layers (Jones, 1975). The rigidities with two subscripts, and more than two subscripts correspond to the classical and shear deformation beam theories, respectively [18].

$$\bar{Q}_{11} = Q_{11} \cos^4 \theta + 2(Q_{12} + 2Q_{66}) \sin^2 \theta \cos^2 \theta + Q_{22} \sin^4 \theta \quad (6)$$

$$\bar{Q}_{55} = Q_{44} \sin^4 \theta + Q_{55} \cos^4 \theta$$

The reduced stiffness parameters depend on the mechanical properties such as elasticity modulus “E”, shear modulus “G” and Poisson's ratio “ $\nu$ ”, and are given as follows:

$$Q_{11} = \frac{E_1}{1 - \nu_{12}\nu_{21}}, \quad Q_{12} = Q_{21} = \frac{E_2\nu_{21}}{1 - \nu_{12}\nu_{21}}, \quad Q_{22} = \frac{E_2}{1 - \nu_{12}\nu_{21}} \quad (7)$$

$$Q_{44} = G_{23}, \quad Q_{55} = G_{13}, \quad Q_{66} = G_{12}$$

$$\frac{E_1}{E_2} = \frac{\nu_{12}}{\nu_{21}} \quad (8)$$

By the appropriate use of stress-strain relations in the force and moment equations,

$$N_x = \int_{-h/2}^{h/2} \sigma_x dz, \quad Q_x^a = \int_{-h/2}^{h/2} \tau_{xz} \Phi^*(z) dz \quad (9)$$

$$M_x = \int_{-h/2}^{h/2} \sigma_x z dz, \quad M_x^a = \int_{-h/2}^{h/2} \sigma_x \Phi(z) dz$$

the following constitutive equations are obtained. “a” corresponds to the shear deformation effects, “A”, “B”, “D” denote the extensional, coupling and bending rigidities respectively, and “ $Q_x^a$ ” “ $Q_x$ a” is the shear force. Rigidities

with two subscripts correspond to the classical theory, whereas the ones with more than two subscripts correspond to shear deformation theory.

$$\begin{bmatrix} N_x \\ M_x \\ M_x^a \end{bmatrix} = \begin{bmatrix} A_{11} & B_{11} & B_{111} \\ B_{11} & D_{11} & D_{111} \\ B_{111} & D_{111} & D_{1111} \end{bmatrix} \begin{bmatrix} u_{,x} \\ -w_{,xx} \\ u_{1,x} \end{bmatrix}, \quad Q_x^a = A_{55} u_1 \quad (10)$$

The extensional, coupling and bending rigidities are defined as follows:

$$A_{11} = \int_{-h/2}^{h/2} \bar{Q}_{11}^{(k)} dz, \quad A_{55} = \int_{-h/2}^{h/2} \bar{Q}_{55}^{(k)} (\mathcal{O}'(z))^2 dz$$

$$B_{11} = \int_{-h/2}^{h/2} \bar{Q}_{11}^{(k)} z dz, \quad B_{111} = \int_{-h/2}^{h/2} \bar{Q}_{55}^{(k)} \mathcal{O}(z) dz \quad (11)$$

$$D_{11} = \int_{-h/2}^{h/2} \bar{Q}_{11}^{(k)} z^2 dz, \quad D_{111} = \int_{-h/2}^{h/2} \bar{Q}_{11}^{(k)} \mathcal{O}(z) z dz,$$

$$D_{1111} = \int_{-h/2}^{h/2} \bar{Q}_{11}^{(k)} (\mathcal{O}(z))^2 dz$$

For a laminated beam under a uniform transverse loading of  $q(x)$ , the governing equations can be considered as follows:

$$N_{x,x} = 0$$

$$M_{x,xx} = q(x) \quad (12)$$

$$M_{x,x}^a - Q_x^a = 0$$

The beam is considered to be under a uniform sinusoidal loading where “m” is the wave number, and given as follows:

$$q(x) = q_0 \sin(\alpha x), \quad \alpha = \frac{m\pi}{L} \quad (m = 1, 2, \dots) \quad (13)$$

The boundary conditions prescribed at both ends where  $x=0$  and  $x=L$ , are obtained by application of Hamilton's principle, and given for simply supported, cantilever and free boundary conditions respectively.

$$N_x = w = M_x = M_x^a = 0$$

$$u = w = w_{,x} = u_1 = 0 \quad (14)$$

$$N_x = M_{x,x} = M_x = M_x^a = 0$$

In order to satisfy the simple support boundary condition, the following Navier-type displacement functions are used, whereas “ $C_1$ ”, “ $C_2$ ” and “ $C_3$ ” are the amplitudes of the displacement functions.

$$u = C_1 \sin\left(\frac{m\pi x}{L}\right), \quad u_1 = C_2 \cos\left(\frac{m\pi x}{L}\right), \quad w = C_3 \sin\left(\frac{m\pi x}{L}\right) \quad (15)$$

Using the constitutive equations in governing equations, the set of three equations with three unknowns are obtained. The unknown parameters can be determined computationally when the boundary condition is applied at both ends.

## FINITE ELEMENT MODEL

In recent years, it has been observed that the use of computer-aided design software is insufficient especially in determining the static and dynamic loads, and the thermal effects of the designs under specific operating conditions. Since the performance of the design will largely depend on the actual operating conditions, it is of great importance to predict these conditions correctly. Under the consideration of these parameters, it will be wise to use a different software solution in the analysis of engineering designs. In the design process, a CAE software is generally used to include the real operating conditions and to create a simulation and perform the analysis in a virtual environment. The CAE software is commonly used in many engineering fields such as automotive, aerodynamic, flow and structural analysis. Especially in the engineering applications, the optimum results can be obtained in a shorter time with the minimum cost. While the design process of a product or system is independent of time and operating conditions, the same parameters should also be taken into consideration in the analysis. The reliability of the results will largely depend on the correct use of the solution technique and the limit values. Thus, the theoretical information in the relevant study becomes significant in the determination of these values. Therefore, especially in cases where the theoretical information is incorrect or insufficient, CAE software may not give the correct or sufficient results. Number of different analyses such as static strength, fatigue, vibration, heat transfer and impact can be performed by use of the finite element method (FEM) based engineering software. As a result, the CAE software shortens the time required for the design process considerably and allows to analyze and predict the optimum results for the product or system before the manufacturing process. In this study, Abaqus is utilized for the CAE solution. Since the plane and shell elements are generally effective in modelling and analyzing the laminated composite structures and converge faster, 3-D brick elements are chosen for the solid modelling.

## RESULTS AND DISCUSSION

The vertical and longitudinal displacements and the shear and normal stresses, namely, the bending stresses are presented in Table 1 at different points. The vertical and longitudinal displacement values are obtained at  $x=L/2$ ,  $z=0$  and  $x=0$ ,  $z=h/2$ , respectively. The normal stresses are obtained at  $x=L/2$ ,  $z=h/4$ , whereas the shear stresses are obtained at  $x=L/4$ ,  $z=0$  in accordance with Ref. [15].

The beam is simply supported, constructed of four layers, has the stacking sequence of  $[90^\circ/0^\circ/0^\circ/90^\circ]$ , length of  $L=6.35$  m, thickness of  $h=2.794$  m and a uniform sinusoidal distributed loading  $q_0=1000$  N/m is applied at the top. The beam material is chosen as boron/epoxy with the following mechanical properties [19]:

$$\begin{aligned} E_{11} &= 241.5 \text{ GPa}, & E_{22} &= E_{33} = 18.89 \text{ GPa} \\ G_{23} &= 3.45 \text{ GPa}, & G_{12} &= G_{13} = 5.18 \text{ GPa} \\ \nu_{23} &= 0.25, & \nu_{12} &= \nu_{13} = 0.24 \end{aligned} \quad (16)$$

The results are compared with Karama et al (1998) that were obtained by Abaqus software [20]. The vertical and longitudinal displacements and bending stresses were also obtained by use of a sinusoidal and exponential shape functions in Karama et al (1998, 2003), and a parabolic shape function in Karacam (2005) [21], respectively. In the present study, the numerical results have shown that the proposed model has better results than the others. In the determination of the displacement and stress values, a unified shear deformation beam theory in which the previous beam theories can be obtained by use of an appropriate shape function, is adopted in the numerical model. In the comparison of results, the following equation is used to obtain the error in percentage.

$$Error(\%) = \frac{(Reference\ Value - New\ Value)}{Reference\ Value} \times 100 \quad (17)$$

**Table 1.** The vertical (W) and longitudinal (U) displacements, shear ( $\tau_{xz}$ ) and normal ( $\sigma_{xx}$ ) stresses for simple support boundary condition.

| Model          | W ( $\times 10^{-4}$ ) [m] | U ( $\times 10^{-4}$ ) [m] | $\tau_{xz}$ [Pa] | $\sigma_{xx}$ [Pa] |
|----------------|----------------------------|----------------------------|------------------|--------------------|
| Present Study  | -6.2155                    | 2.3554                     | -1031670         | 7685460            |
| Error (%)      | 1.88                       | 1.85                       | 2.55             | 1.91               |
| Karacam (2005) | -6.2317                    | 2.0382                     | -892316          | 7527000            |
| Error (%)      | 2.2                        | 11.8                       | 11.3             | 3.9                |
| Karama (2003)  | -6.3701                    | 2.1196                     | -940098          | 8112840            |
| Error (%)      | 4.4                        | 8.3                        | 6.6              | 3.5                |
| Karama (1998)  | -6.1006                    | 2.3125                     | -1006000         | 7835200            |

In Fig. 2, the variation of vertical displacement is presented along the beam length. In accordance with the simply support boundary condition, the displacement values at the beginning and end of the beam where  $x=0$  and  $x=L$ , are obtained as zero. The maximum displacement value is obtained in the middle of the beam as it is expected. Due to the sinusoidal transverse loading, the negative values in the vertical axis indicate that the displacement values are obtained in the negative z- direction.

In Fig. 3, the vertical displacement distribution is presented. It is obvious from the figure that both sides of the beam which are illustrated in red regions have zero displacement, whereas the regions in dark blue correspond to the maximum displacement values.

In Fig. 4, the variation of longitudinal displacement along the beam thickness is presented. Since the sinusoidal loading acts from the top, the upper surface of the beam is

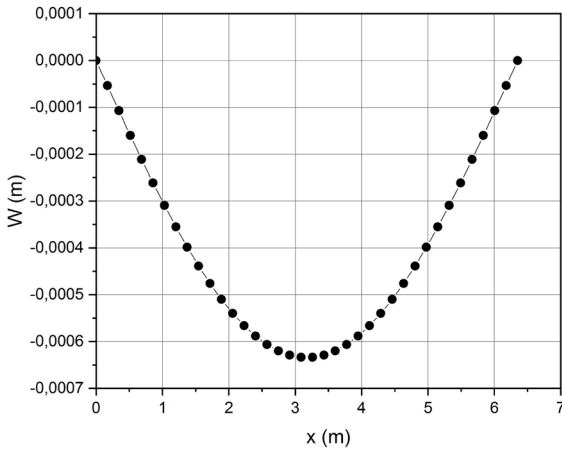


Figure 2. The variation of vertical displacement along the beam length.

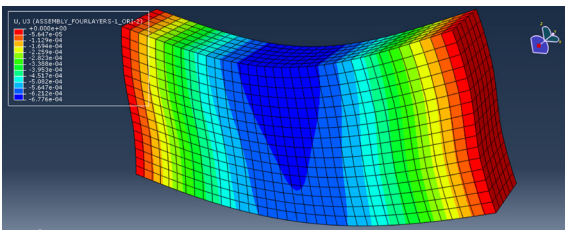


Figure 3. The vertical displacement distribution.

lengthened, whereas the lower surface is shorten. Thus, the maximum values are obtained at the bottom and top surfaces where  $z=h/2$  and  $z=-h/2$ . The longitudinal displacement values presented along x-axis in the figure have a common factor of “ $10^{-4}$ ”. Since the longitudinal displacement at the mid-plane of the beam when  $z=0$  is “ $0.06 \times 10^{-4}$ ”, it is obvious from the figure that the displacement at this value is very close to zero.

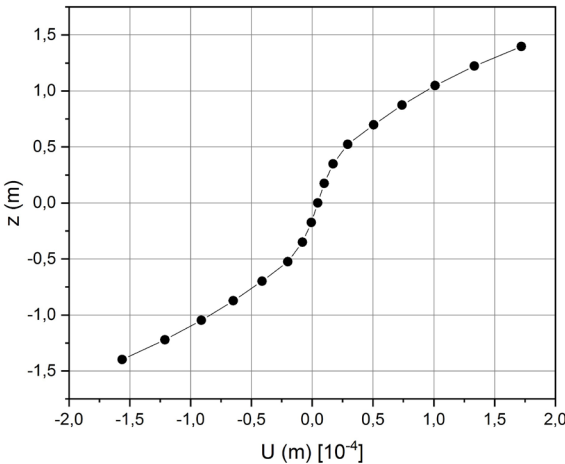


Figure 4. The variation of longitudinal displacement along the beam thickness.

The longitudinal displacement distribution along the beam thickness is presented in Fig. 5. The red and dark blue regions indicate the positive and negative maximum displacement values at the bottom and top surfaces along x-axis.

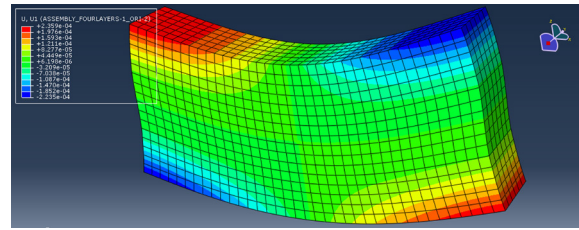


Figure 5. The longitudinal displacement distribution.

In the mid-plane, the longitudinal displacement values are close to zero as in the previous figure.

In Fig. 6, the variation of normal stress along the beam length is presented. The maximum value is obtained in the mid-point, and stress values are obtained as zero at both ends of the beam respectively.

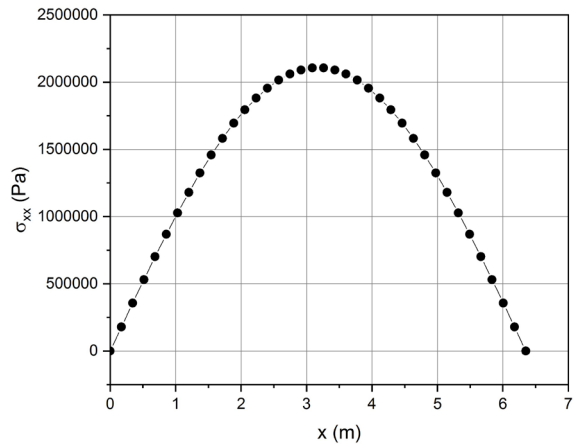


Figure 6. The variation of normal stress along the beam length.

In Fig. 7, the normal stress distribution along the beam length is presented. For the specific point where  $x=L/2$  and  $z=h/4$ , the stress values are close to the analytical solution. The positive and negative stress values correspond to the tensile and compressive stresses.

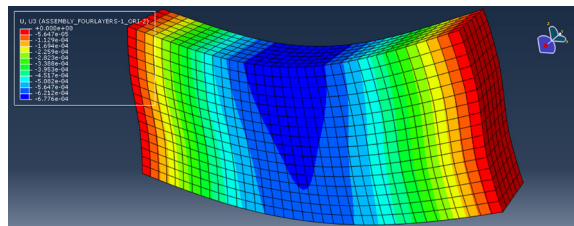


Figure 7. The normal stress distribution.

In Fig. 8, the variation of shear stress along the beam thickness is presented. At the bottom and top surfaces, the shear stresses are obtained as zero in accordance with the shear deformation beam theory, and the maximum stress value is obtained in the mid-plane.

In Fig. 9, the shear stress distribution along the beam thickness is presented. The stress values are close to the refe-

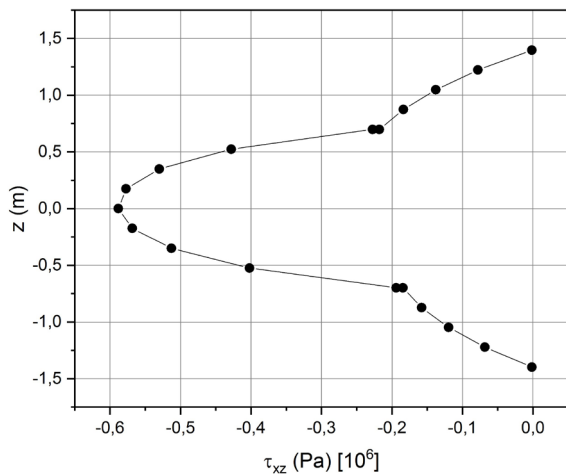


Figure 8. The variation of the shear stress along the beam thickness.

rence values where  $x=L/4$ , and  $z=0$ . The colored regions are similar with the curve obtained by the analytical solution in the previous figure.

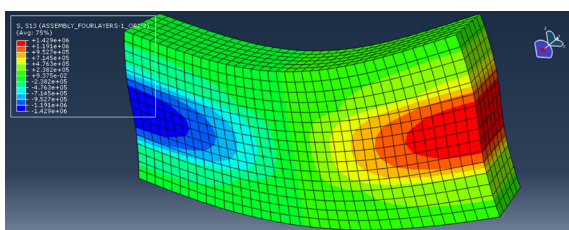


Figure 9. The shear stress distribution.

## CONCLUSION

In this study, the bending analysis of a composite beam under a uniform sinusoidal load is performed. By use of the proposed model, the results are compared with the analytical and CAE solutions of the previous studies. When the results are compared with the reference values, the percentage values of errors are obtained as 1.88% and 1.85% for vertical and longitudinal displacements, 2.55% and 1.91% for the shear and normal stresses, respectively. Thus, it is concluded from the results that there is a significant decrease in percentage error values from 11.8% and 11.3% for the longitudinal displacement and shear stress values, whereas there is a minor change from 2.2% and 3.9% for the vertical displacement and normal stress values when compared with the analytical solution of Karacam, 2005. In the future works, the dynamic analysis can be performed in order to obtain the natural frequencies and buckling loads. Additionally, the static and dynamic analyses can be expanded by taking various design parameters into consideration such as loading type, stacking sequence, layer thickness and boundary conditions.

## CONFLICT OF INTEREST

The author deny any conflict of interest.

## REFERENCES

1. Sankar BV. An elasticity solution for functionally graded beams. *Composites Science and Technology*. 2001;61:689–696.
2. Sayyad AS, Ghugal YM, Borkar RR. Flexural analysis of fibrous composite beams under various mechanical loadings using refined shear deformation theories. *Composites: Mechanics, Computations, Applications. An International Journal*. 2014;5(1):1–19.
3. Sayyad AS, Ghugal YM, Naik NS. Bending analysis of laminated composite and sandwich beams according to refined trigonometric beam theory. *Curved and Layered Structures*. 2015;2:279–289.
4. Pimenta RJ, Queiroz G, Diniz SMC. Reliability-based design recommendations for sinusoidal-web beams subjected to lateral-torsional buckling. *Engineering Structures*. 2015;84:195-206.
5. Pagani A, Yan Y, Carrera E. Exact solutions for static analysis of laminated, box and sandwich beams by refined layer-wise theory. *Composites Part B*. 2017;13:62–75.
6. Jiaoa P, Borchania W, Soleimania S, McGraw B. Lateral-torsional buckling analysis of wood composite I-beams with sinusoidal corrugated web. *Thin-Walled Structures*. 2017;119:72-82.
7. Liu T, Li ZM, Jin S. Nonlinear bending analysis of anisotropic laminated tubular beams based on higher-order theory subjected to different kinds of distributed loads. *International Journal of Pressure Vessels and Piping*. 2018;163:23–35.
8. Dorduncu M. Stress analysis of laminated composite beams using refined zigzag theory and peridynamic differential operator. *Composite Structures*. 2019;218:193–203.
9. Karakoti A, Kar VR. Deformation characteristics of sinusoidally-corrugated laminated composite panel – A higher-order finite element approach. *Composite Structures*. 2019;216:151–158.
10. PandeyN, GadadeAM. Static response of laminated composite beam subjected to transverse loading. *Materials Today: Proceedings*. 2019;16:956–963.
11. Sobhy M. Levy solution for bending response of FG carbon nanotube reinforced plates under uniform, linear, sinusoidal, and exponential distributed loadings. *Engineering Structures*. 2019;182:198–212.
12. Wang M, Xu YG, Qiao P, Li ZM. A two-dimensional elasticity model for bending and free vibration analysis of graphene-reinforced composite laminated beams. *Composite Structures*. 2019;211:364–375.
13. Pathirana S, Qiao P. Local buckling analysis of periodic sinusoidal corrugated composite panels under uniaxial compression. *Composite Structures*. 2019;220:148–157.
14. Pathirana S, Qiao P. Elastic local buckling of periodic sinusoidal corrugated composite panels subjected to in-plane shear. *Thin-Walled Structures*. 2020;157:107134.
15. Zaboon JK, Jassim SF. Bending of cross-ply laminated composite beams with various boundary conditions and loading. *Materials Today: Proceedings*. 2022;61:930-934.

16. Zhu S, Zhang YX, Lee CK. Experimental investigation of flexural behaviours of hybrid engineered cementitious composite beams under static and fatigue loading. *Engineering Structures*. 2022;262:114369.
17. Soldatos KP, Timarci, T. A unified formulation of laminated composite, shear deformable five-degrees-of-freedom cylindrical shell theories. *Composite Structures*. 1993;25:165-171.
18. Jones RM. *Mechanics of Composite Materials*. McGraw-Hill New York; 1975.
19. Karama M, Afaq KS, Mistou S. Mechanical behaviour of laminated composite beam by the new multi-layered laminated composite structures model with transverse shear stress continuity. *International Journal of Solids and Structures*. 2003;40:1525-1546.
20. Karama M, Harb BA, Mistou S, Caperaa S. Bending, buckling and free vibration of laminated composite with a transverse shear stress continuity model. *Composites Part B*. 1998;29(B):223-234.
21. Karacam F, Timarci T. Bending of cross-ply beams with different boundary conditions. UNITECH Gabrovo-05 International Scientific Conference, Gabrovo, Bulgaria, November. 2005;2:137-142.